Microfibrous Chitosan−Sepiolite Nanocomposites

Margarita Darder,[†] Mar López-Blanco,[†] Pilar Aranda,[†] Antonio J. Aznar,[‡] Julio Bravo,[‡] and Eduardo Ruiz-Hitzky*,[†]

Instituto de Ciencia de Materiales de Madrid, CSIC, Cantoblanco, 28049-Madrid, Spain, and Departamento de Ciencia e Ingeniería de Materiales e Ingeniería Química, Universidad Carlos III de Madrid, Avda. Universidad, 30, 28911-Leganés, Spain

Received October 27, 2005. Revised Manuscript Received December 21, 2005

We report in this paper the synthesis and characterization of a new class of biopolymer−clay nanocomposites based in the assembling of chitosan to sepiolite, which is a natural magnesium silicate showing a microfibrous texture. CHN and ICP/AES chemical analyses, XRD, FTIR spectroscopy, ^{13}C solid-state NMR, LT-SEM, and thermal analysis have been employed in the characterization of the resulting nanocomposites. The adsorption isotherm of chitosan on sepiolite in acidic medium reveals a significant coverage of the biopolymer at high equilibrium concentration values indicating a multilayer adsorption. The arrangement of chitosan chains on the surface of the silicate microfibers is discussed on the basis of physicochemical data obtained by application of the different techniques. The potentiometric response of this new type of bio-nanocomposites incorporated in carbon paste electrodes toward aqueous salt solutions was employed for the first time as a valuable technique for a rapid assessment of the ion-exchange behaviors. Thermal behaviors and mechanical properties have been determined by DTA-TG and DMTA, respectively. As these materials are well-processed as self-supporting films, in view of their properties they show potential interest as membranes for different processes related to separation of ions and gases, as well as components in electrochemical devices (fuel-cell, potentiometric sensors).

Introduction

The increasing interest in the preparation of polymer−clay nanocomposites relies on the good properties of these hybrid materials resulting from the synergic effect of the interaction of both components at the nanometric scale.[1] Within this research field, the development of biohybrid nanostructured materials has begun to receive special attention in recent years.[2,3] Nature offers good examples of this kind of material, for instance nacre[4] and ivory.[5] A current trend in materials science involves the development of biomimetic or bioinspired materials[6] based on the combination of natural polymers with inorganic solids, including clay minerals. In this way, 2:1 layered silicates have been combined with cationic biopolymers such as chitosan,[7] gelatin,[8] and poly-L-lysine,[9] while layered double hydroxides (LDHs) interact with negatively charged polymers including pectin, alginate, carrageenan,[10] DNA,[11] or poly(α,β-aspartate)[12] giving rise to different type of bio-nanocomposites. The resulting nanostructured biohybrid materials are envisaged for many different applications, from tissue engineering

[†] Instituto de Ciencia de Materiales de Madrid.
[‡] Universidad Carlos III de Madrid.
* To whom correspondence should be addressed. Fax: +34-91-3720623. E-mail: eduardo@icmm.csic.es.

(1) (a) Tuney, J. J.; Detellier. C. *Chem. Mater.* **1996**, *8*, 927−935. (b) Lagaly, G. *Appl. Clay Sci.* **1999**, *15*, 1−9. (c) Pinnavaia, T. J., Beall, G. W., Eds.; *Polymer-Clay Nanocomposites*; John Wiley & Sons: West Sussex, 2000. (d) Carrado, K. A. *Appl. Clay Sci.* **2000**, *17*, 1−23. (e) Ruiz-Hitzky, E.; Aranda, P.; Serratosa, J. M. Clay Organic Interactions: Organoclay Complexes and Polymer-Clay Nanocomposites. In *Handbook of Layered Materials*; Auerbach, S. M., Carrado, K. A., Dutta, P. K., Eds.; Marcel Dekker: New York, 2004; pp 91−154. (f) Sanchez, C.; Julian, B.; Belleville, P.; Popall, M. *J. Mater. Chem.* **2005**, *15*, 3559−3592.

(2) Ruiz-Hitzky, E. *Chem. Rec.* **2003**, *3*, 88−100.

(3) (a) Ruiz-Hitzky, E.; Darder, M.; Aranda, P. *J. Mater. Chem.* **2005**, *15*, 3650−3662. (b) Ruiz-Hitzky, E.; Aranda, P.; Darder, M. In *Bottom-Up Nanofabrication: Supramolecules, Self-Assemblies, and Organized Films*; Ariga, K., Ed.; American Scientific Publishers (in press).

(4) (a) Zaremba, C. M.; Morse, D. E.; Mann, S.; Hansma, P. K.; Stucky, G. D. *Chem. Mater.* **1998**, *10*, 3813−3824. (b) Smith, B. L.; Schaeffer, T. E.; Viani, N.; Thompson, J. B.; Frederick, N. A.; Kindt, J.; Belcher, A.; Stucky, G. D.; Morse, D. E.; Hansma, P. K. *Nature* **1999**, *399*, 761−763. (c) Schaeffer, T. E.; Ionescu-Zanetti, C.; Proksch, R.; Fritz, M.; Walters, D. A.; Almqvist, N.; Zaremba, C. M.; Belcher, A. M.; Smith, B. L.; Stucky, G. D.; Morse, D. E.; Hansma, P. K. *Chem. Mater.* **1997**, *9*, 1731−1740.

(5) Su, X. W.; Cui, F. Z. *Mater. Sci. Eng. C* **1999**, 7, 19−29.

(6) (a) Sellinger, A.; Weiss, P. M.; Nguyen, A.; Lu, Y.; Assink, R. A.; Gong, W.; Brinker, C. J. *Nature* **1998**, *394*, 256−260. (b) Almqvist, N.; Thomson, N. H.; Smith, B. L.; Stucky, G. D.; Morse, D. E.; Hansma, P. K. *Mater. Sci. Eng. C* **1999**, *7*, 37−43. (c) Tang, Z.; Kotov, N. A.; Magonov, S.; Ozturk, B. *Nature Mater.* **2003**, *2*, 413−418.

(7) (a) Darder, M.; Colilla, M.; Ruiz-Hitzky, E. *Chem. Mater.* **2003**, *15*, 3774−3780. (b) Darder, M.; Colilla, M.; Ruiz-Hitzky, E. *Appl. Clay Sci.* **2005**, *28*, 199−208.

(8) (a) Talibudeen, O. *Nature* **1950**, *166*, 236−236. (b) Weiss, A. Organic derivatives of clay minerals, zeolites and related minerals. In *Organic Geochemistry*; Eglinton G., Murphy, M. T. J., Eds.; Springer-Verlag: Berlin, 1969; pp 737−781. (c) Zheng, J. P.; Li, P.; Ma, Y. L.; Yao, K. D. *J. Appl. Polym. Sci.* **2002**, *86*, 1189−1194. (d) Li, P.; Zheng, J. P.; Ma, Y. L.; Yao, K. D. *J. Appl. Polym. Sci.* **2003**, *88*, 322−326. (e) Darder, M.; Ruiz, A. I.; Aranda, P.; Van Damme, H.; Ruiz-Hitzky, E. *Corr. Nanosci.* (in press.)

(9) Krikorian, V.; Kurian, M.; Galvin, M. E.; Nowak, A. P.; Deming, T. J.; Pochan, D. J. *J. Polym. Sci. B: Polym. Phys.* **2002**, *40*, 2579−2586.

(10) Darder, M.; López-Blanco, M.; Aranda, P.; Leroux, F.; Ruiz-Hitzky, E. *Chem. Mater.* **2005**, *17*, 1969−1977.

(11) (a) Choy, J. H.; Kwak, S. Y.; Park, J. S.; Jeong, Y. J.; Portier, J. *J. Am. Chem. Soc.* **1999**, *121*, 1399−1400. (b) Choy, J. H.; Kwak, S. Y.; Jeong, Y. J.; Park, J. S. *Angew. Chem., Int. Ed.* **2000**, *39*, 4042−4045. (c) Kwak, S. Y.; Jeong, Y. J.; Park, J. S.; Choy, J. H. *Solid State Ionics* **2002**, *151*, 229−234.

(12) Whilton, N. T.; Vickers, P. J.; Mann, S. *J. Mater. Chem.* **1997**, *7*, 1623−1629.

10.1021/cm0523642 CCC: $33.50
Published on Web 02/16/2006

Scheme 1. Idealized Representation of Chitosan Adsorption on the Sepiolite Surface

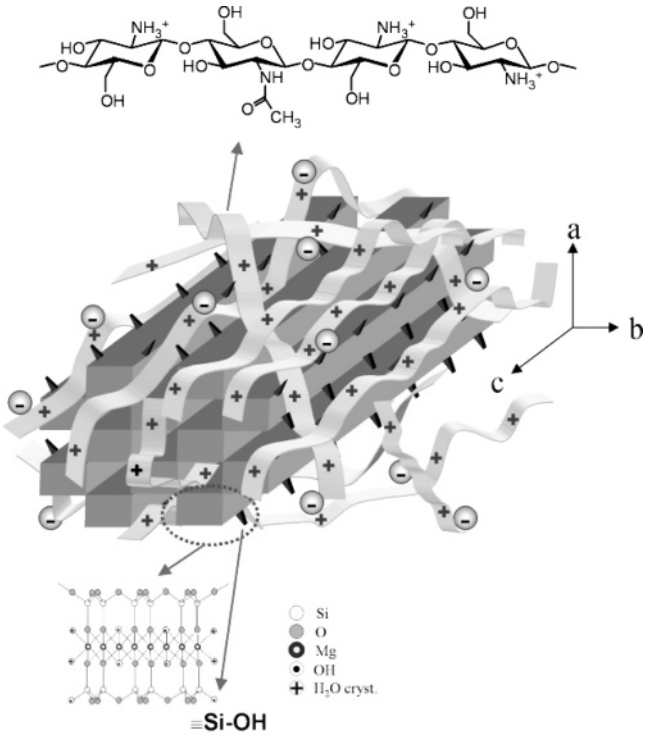

in biomedicine to food packaging or drinking water purification, due to the special properties afforded by the organic moiety regarding biocompatibility and biodegradability. In addition to the above-mentioned layered silicates and following a similar approach, sepiolite has been also employed as a substrate for the adsorption of collagen[13] in order to prepare biocompatible hybrid materials suitable as scaffolds for bone repair purposes.[14]

The clay mineral sepiolite is a microcrystalline hydrated magnesium silicate of theoretical unit cell formula $Si_{12}O_{30}Mg_8(OH,F)_4(H_2O)_4 \cdot 8H_2O$. It exhibits a microfibrous morphology and a particle size in the 2−10 μm length range.[15] Sepiolite shows an alternation of blocks and tunnels that grow up in the fiber direction (Scheme 1). The blocks are constituted by two layers of tetrahedral silica sandwiching a central magnesium oxide−hydroxide layer, and the dimensions of the cross-section of tunnels are about 1.1×0.4 nm^2. The discontinuity of the silica sheets gives rise to the presence of silanol groups (Si−OH) at the edges of the channels, which are the tunnels opened to the external surface of the sepiolite particles.[16] Tunnels are filled with both the coordinated water molecules, which are bonded to the Mg^{2+} ions located at the edges of octahedral sheets, and the zeolitic water, which is associated to the former by hydrogen bonding.

Sepiolite has been described as a clay mineral showing the ability to give polymer−clay nanocomposites as well as the widely used smectites.[17] Polymers not only interact with the external surface of this silicate, but they can also penetrate into the structural tunnels of the mineral.[18−20] It is well-known that the reinforcement of polymeric matrixes with inorganic fillers of different structure, composition, and morphology depends on the interactions established between both components. Thus, particles with a high aspect ratio are expected to enhance the mechanical properties of the polymeric matrix in the resulting hybrid material. In this way, sepiolite has been recently employed as an anisometric filler for the reinforcement of elastomers, including poly(dimethylsiloxane) and poly(hydroxyethyl acrylate).[21,22] Palygorskite is a related fibrous clay mineral that has been also recently described for preparation of different polymer−clay nanocomposites.[23]

In this work, sepiolite has been combined to chitosan, a natural polysaccharide bearing amino and hydroxyl groups in its structure, to develop nanostructured biohybrid materials provided with enhanced mechanical properties. Chitosan is a biocompatible polymer widely used for numerous applications in different areas: photography, cosmetics, food and nutrition, biomedical purposes, etc.[24] At slightly acidic pH, amino groups in the chitosan structure are protonated making this polysaccharide as a polymeric electrolyte that could be able to compensate the negatively charged sepiolite substrate. In addition to this interaction mechanism, hydrogen bonding can be established between the hydroxyl groups of chitosan and the silanol groups on the external surface of sepiolite. The combination of both types of interactions together with the elevated specific surface area of this silicate (>300 m^2/g) are the bases for choosing sepiolite as substrate for the preparation of new hybrid materials that may exhibit microfibrous morphology and provide attractive mechanical properties as well as ion-exchange behavior.

Experimental Section

Starting Materials and Reagents. Sepiolite (Pangel S9) provided with a cation exchange capacity (CEC) value close to 15 mequiv/100 g was received from TOLSA. Chitosan (high molecular weight; deacetylation degree, DD, of ca. 75%) was supplied by Aldrich. Acetic acid was obtained from Merck and NaCl (ACS reagent) from Riedel-de Haën. Deionized water (resistivity of 18.2 MΩ cm) was obtained with a Maxima Ultrapure Water system from Elga.

(13) Pérez-Castells, R.; Álvarez, A.; Gavilanes, J.; Lizarbe, M. A.; Martínez del Pozo, A.; Olmo, N.; Santaren, J. In *Proceedings of the International Clay Conference, Denver*; Schultz, L. G., van Olphen, H., Mumpton, F. A., Eds.; The Clay Minerals Society: Bloomington, IN, 1985; pp 359−362.
(14) (a) Olmo, N.; Lizarbe, M. A.; Gavilanes, J. G. *Biomaterials* **1987**, *8*, 67−69. (b) Olmo, N.; Turnay, J.; Herrera, J. I.; Gavilanes, J. G.; Lizarbe, M. A. *J. Biomed. Mater. Res.* **1998**, *30*, 77−84.
(15) (a) Brauner, K.; Preisinger, A. *Miner. Petr. Mitt.* **1956**, *6*, 120−140. (b) Santarén, J.; Sanz, J.; Ruiz-Hitzky, E. *Clay Miner.* **1990**, *38*, 63−68.
(16) Ahlrichs, J. L.; Serna, J. C.; Serratosa, J. M. *Clays Clay Miner.* **1975**, *23*, 119−124.
(17) Ruiz-Hitzky, E.; Van Meerbeek, A. In *Handbook of Clay Science*; Bergaya, F., Theng, B. K. G., Lagaly, G., Eds.; Elsevier: Chapter 10.3 (in press).
(18) Inagaki, S.; Fukushima, Y.; Miyata, M. *Res. Chem. Interm.* **1995**, *21*, 167−180.
(19) Sandi, G.; Carrado, K. A.; Winans, R. E.; Johnson, C. S.; Csencsits, R. *J. Electrochem. Soc.* **1999**, *146*, 3644−3648.
(20) Ruiz-Hitzky, E. *J. Mater. Chem.* **2001**, *11*, 86−91.
(21) González Hernández, L.; Ibarra Rueda, L.; Rodríguez Díaz, A.; Chamorro Antón, C. *Angew. Makromol. Chem.*, **1982**, *103*, 51−60.
(22) (a) Bokobza, L. *J. Appl. Polym. Sci.* **2004**, *93*, 2095−2104. (b) Bokobza, L.; Burr, A.; Garnaud, G.; Perrin, M. Y.; Pagnotta, S. *Polym. Int.* **2004**, *53*, 1060−1065.
(23) Wang, L.; Sheng, J. *Polymer* **2005**, *46*, 6243−6249.
(24) Ravi Kumar, M. N. V. *React. Funct. Polym.* **2000**, *46*, 1−27.

Synthesis Procedure. Sepiolite suspension (3% w/v) was prepared in bidistilled water, and a vigorous stirring was applied by means of a mixer (G2 model, Lomi) in order to properly disperse the clay. Different amounts of chitosan were dissolved in 50 mL of 1% v/v acetic acid in order to prepare a set of aqueous solutions with chitosan concentrations ranging between 0.804 and 30 g L^{-1}. Each chitosan solution was added to 50 mL of the sepiolite dispersion, and the mixture was stirred for 24 h at room temperature. To prepare films of the chitosan−sepiolite nanocomposites, an aliquot of the sepiolite/chitosan mixture (7.6 mL) was vacuum filtered onto a Millipore membrane (0.025 μm of pore diameter), and the resulting films of sepiolite with an excess of chitosan were allowed to dry overnight at room temperature. These films were denoted as "non-washed nanocomposite" (N-WN) samples. Other aliquots of the chitosan−sepiolite suspensions were centrifuged, and the supernatants were kept. The solid fractions were washed three times with bidistilled water in order to reach a neutral pH value. These "washed nanocomposite" (WN) samples were then re-dispersed in bidistilled water in order to prepare films of sepiolite without excess of chitosan following the aforementioned procedure.

Characterization. The resulting chitosan−sepiolite nanocomposites were characterized by chemical analysis (Perkin-Elmer 2400 CHN analyzer), XRD (Bruker D8 instrument with a Cu anode and Ni filter), thermal analysis (TG and DTA) (SSC/5200 Seiko analyzer), IR spectroscopy (Nicolet 20SXC spectrophotometer), and inductively coupled plasma/atomic emission spectrometry (ICP/AES) (Perkin-Elmer, Plasma 40). ^{13}C CP MAS NMR spectra were obtained in a Bruker Avance 400 spectrometer, using a standard cross-polarization pulse sequence. Samples were spun at 10 kHz. Spectrometer frequencies were set to 100.62 and 400.13 MHz for ^{13}C and ^{1}H, respectively. A contact time of 2 ms and a period between successive accumulations of 5 s were used. The number of scans was 800. Chemical shift values were referenced to tetramethylsilane (TMS).

For low-temperature scanning electron microscopy (LT-SEM), a drop of each aqueous chitosan−sepiolite sample was deposited on the specimen holder of a cryotransfer system at room temperature. The drops were immediately plunged-frozen in slush nitrogen and directly transferred into the cryochamber, pre-cooled to −180 °C via an air-lock transfer device. The frozen drop was then fractured with a cooled blade, and an etching process was applied by slowly heating the chamber to −90 °C over a 2 min period. This process allows sublimation of the first superficial micrometers of water. The etched fragment was returned to the cryochamber, sputter-coated with gold for 2 min 15 s at 10 mA, and then moved to the SEM chamber pre-cooled to −150 to −160 °C where it was observed at an acceleration voltage of 10−15 kV. The instrument used was a CT 1500 Cryotrans system (Oxford Instruments) mounted on a ZEISS DSM-960 microscope.

To check the ion-exchange capacity of the chitosan−sepiolite samples, modified carbon paste electrodes (CPEs) were prepared by thoroughly mixing 20 mg of each chitosan−sepiolite nanocomposite, 40 mg of graphite powder (1−2 μm, synthetic, from Aldrich), and 40 mg of paraffin oil as liquid binder in an agate mortar. The modified carbon paste was then packed firmly into the cavity of an electrode body (internal diameter 3 mm), and the electrical contact was established by a copper wire. The electrode surface was polished on paper until a smooth surface was obtained. Potentiometric measurements were performed with an Orion EA920 ion selective meter. The homemade sensors acted as the working electrode in a conventional two-electrode configuration, and the potential was measured (at room temperature) against a Ag/AgCl reference electrode.

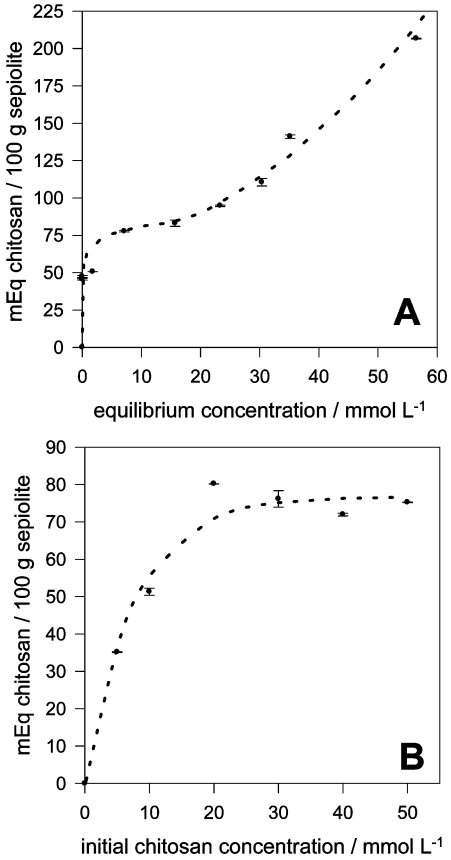

Figure 1. Adsorption isotherm at 25 °C of chitosan onto sepiolite obtained for N-WN samples (A) and adsorbed chitosan amounts measured in the WN samples (B). Adsorption amounts were deduced from CHN chemical analyses.

The mechanical properties of the samples were determined using a dynamic mechanical thermal analyzer (DMTA Mk-III Rheometric Scientific) by Polymer Laboratories Ltd. The DMTA measurement unity was positioned on horizontal drive shaft orientation, and the samples were loaded horizontally using small size bending clamps. The measurements were performed at 22 °C. All samples were cut to dimensions of 15 × 6 mm^2 from films of different thickness prepared previously. Samples were inserted symmetrically and horizontally into the clamp assembly, fixing the sample free length to 5 mm. The full calibration procedure was followed before each measurement session. The samples were stretched with incremental force. The total force is a function of the thickness, the width, and the mechanical properties of the samples, and it was calculated for each one to finish the experiment before the breaking of the sample takes place. The elasticity moduli were obtained from the slope of the linear zone of the stress−strain curves.

Results and Discussion

Synthesis and Characterization. In both types of samples, N-WN and WN, electrostatic interactions in acidic medium between the positively charged amino groups of chitosan and the negatively charged sepiolite are established. In addition, a considerable interaction is expected between hydroxyl groups belonging to the biopolymer structure and the silanol groups present on the external surface of sepiolite (Scheme 1).

The adsorption isotherm of chitosan (25 °C) from water solutions was determined from CHN chemical analyses indicating that multilayer adsorption takes place (Figure 1A).

According to the Giles classification of isotherms,[25] it can be defined as a H-type isotherm, a special case of the L-type curve, indicating a high affinity between the sepiolite substrate and the biopolymer adsorbate, being the chitosan completely adsorbed from dilute solutions. The formation of molecular aggregates on the silicate surface is favored by the great affinity between chitosan due to intermolecular hydrogen bonding interactions. By washing the samples, i.e., after elimination of most of the aggregated chitosan ("excess"), the maximum amount of adsorbed chitosan results in 75 mequiv/100 g of sepiolite (Figure 1B), which largely overpasses the CEC value of sepiolite (ca. 15 mequiv/100 g).

Considering an average area of glucosamine and *N*-acetylglucosamine units in the chitosan chain of 55×10^{-20} m^2,[2,26] the adsorbed amount of chitosan in the plateau of WN samples would be covering a total area of about 260 m^2/g by supposing a full planar disposition of unfolded biopolymer chains. Taking into account that the specific surface area (BET, N_2) of the starting sepiolite is 335 m^2/ g,[20] it can be estimated that a large part of that surface is covered by the biopolymer. As the starting silicate exhibits a significant pore volume of dimensions only accessible to small molecules, a theoretical coverage of an area value as high as 260 m^2/g would be indicative that the external surface area of the clay (ca. 150 m^2/ g)[20,27] must be completely covered by the chitosan chains. Besides, it should be also considered that a fraction of chitosan could be involved in the partial penetration into the structural tunnels of nanometric dimensions of sepiolite, as it has been also reported for other polymeric chains (PEO) acceding to this type of nanopores.[20] However, such a situation could be strongly restricted because of the steric hindrance of chitosan chains. The specific surface area of WN and N-WN samples is strongly reduced with respect to that of pristine sepiolite, giving rise to values in the 160−200 m^2/g range, indicating that chitosan is homogeneously disposed on the silicate surface avoiding the access of nitrogen to the nanopores during the BET measurements.

The preparation of chitosan−sepiolite nanocomposites is carried out in the acidic medium required to dissolve the biopolymer. It is known that the treatment of sepiolite by acids produces the magnesium extraction, and therefore a structural alteration could be significant in appropriated experimental conditions.[21,28] The extracted magnesium was measured (ICP/AES) in the supernatant obtained after centrifugation of the chitosan−sepiolite mixtures. For all the preparations the measured amount of lixiviated Mg was ca. 26 mg L^{-1}, which corresponds approximately to 1.4% of the Mg content in the sepiolite. This fact points out that the sepiolite structure is practically unaltered by treatment in the acidic medium during the preparation step. It must be assumed that the presence of chitosan on the mineral surface has a protective effect against the acid attack, similarly to that observed for acid treatment of sepiolite in the presence of organosilanes as protecting agents.[29] In agreement, XRD confirms that the crystal structure of sepiolite is preserved during the nanocomposite preparation procedure (Figure 2B). As expected, the intense peak at 1.10−1.20 nm in the diffractograms of the nanocomposites (Figure 2C−F), attributed to reflections from the (*110*) planes in the sepiolite structure, is not shifted because of the chitosan adsorption. The N-WN samples (Figure 2C,E) obtained from chitosan/sepiolite mixtures with low and high chitosan content (10.7 and 42.9 g per 100 g, respectively) show lower cristallinity than pristine sepiolite, in contrast to the washed samples prepared from the same starting mixtures (Figure 2D,F). This observation can be explained by the high biopolymer content in the N-WN samples, showing a "dilution effect" of sepiolite in the chitosan. Also a preferential orientation of the silicate microcrystals could be proposed in view of the enhancement of reflections at 0.64, 0.44, 0.33, and 0.26 nm, which apparently are rational orders probably related to the layered organization imposed by the biopolymer structure.

The IR spectra in the 4000−550 cm^{-1} wavenumber range of the starting components, chitosan and sepiolite, together with those corresponding to the derived nanocomposites have been included in Figure 3. Chitosan spectrum (Figure 3a) shows the characteristic vibration bands of a polysaccharide bearing amino and acetyl groups ($\nu_{N-H} \sim 3454$ cm^{-1}; $\nu_{O-H} \sim 3364$ cm^{-1}; $\nu_{C-H} \sim 2911$ cm^{-1}; $\nu_{C-H} \sim 2868$ cm^{-1}; amide II ~ 1656 cm^{-1}; $\delta_{NH3} \sim 1580$ cm^{-1}; $\delta_{CH} \sim 1379$ cm^{-1}; $\nu_{C-O} \sim 1153$ cm^{-1}; ν_{C-H} of C−O−C ~ 1072 cm^{-1} characteristic of the piranose ring),[30,31] whereas characteristic bands of the sepiolite (ν_{OH} attributed to zeolitic water $\sim 3650-3400$ cm^{-1}; δ_{HOH} of coordinated water molecules ~ 1666 cm^{-1}; and ν_{SiO} of Si−O−Si ~ 1020 cm^{-1})[32] are shown in Figure 3b.

The nanocomposites prepared from a solution containing initially 42.9 g of chitosan/100 g sepiolite have been chosen to compare the two types of samples, WN (Figure 3c) and N-WN samples (Figure 3d). In the first case, the amount of chitosan that remains adsorbed onto sepiolite after the washing treatment provides bands of very low intensity in comparison to those of sepiolite, being almost unappreciable (Figure 3c). The band attributed to the protonated amino groups is shifted toward 1547 cm^{-1}, confirming the establishment of electrostatic interactions between the silicate surface and the biopolymer.[7,30]

(25) Giles, C. H.; MacEwan, T. H.; Nakhwa, S. N.; Smith, D. *J. Chem. Soc.* **1960**, 3973−3993.
(26) Clark, G. L.; Smith, A. F. *J. Phys. Chem.* **1936**, *40*, 863−879.
(27) Kuang, W. X.; Facey, G. A.; Detellier, C.; Casal, B.; Serratosa, J. M.; Ruiz-Hitzky, E. *Chem. Mater.* **2003**, *15*, 4956−4967.
(28) (a) Aznar, A. J.; Gutiérrez, E.; Díaz, P.; Alvarez, A.; Poncelet, G. *Microporous Mater.* **1996**, *6*, 105−114. (b) Fernández Alvárez, T. *Bol. Soc. Esp. Ceram. Vidrio* **1972**, *11*, 365−374. (c) Aznar Jiménez, A.; Álvarez Berenguer, A.; Díaz del Castillo, P.; Coca Marcos, J.; Poncelet, G. Procedimiento de preparación de una sílice de alta superficie específica. (Procedure for preparation of a silica provided with high specific surface area). Patent P-9002483 (Spain), 1990. (d) Yebra-Rodríguez, A.; Martín-Ramos, J. D.; Rey, F.; Viseras, C.; López-Galindo, A. *Clay Miner.* **2003**, *38*, 353−360. (e) Ozdemir, M.; Kipcak, I. *Clays Clay Miner.* **2004**, *52*, 714−720.
(29) (a) Ruiz-Hitzky, E.; Fripiat, J. J. *Bull. Soc. Chim.* **1976**, 1341−1348. (b) Ruiz-Hitzky, E.; Van Meerbeek, A. *Colloid Polym. Sci.* **1978**, *256*, 135−139.
(30) Yaku, F. Chitosan-metal complexes and their function. In *Proceedings of the First International Conference on Chitin/Chitosan*; Muzzarelli, R. A. A., Pariser, E. R., Eds.; Massachusetts Institute of Technology: Boston, 1978; pp 386−405.
(31) Avram, M.; Mateescu, Gh. D. In *Spectroscopie infrarouge: applications en chimie organique (Infrared spectroscopy: applications in organic chemistry)*; Dunod: Paris, 1970; pp 577−582.
(32) Serratosa, J. M. In *Proceedings of the International Clay Conference, Oxford, 1978*; Mortland, M. M., Farmer, V. C., Eds.; Elsevier Science: Amsterdam, 1979; pp 99−109.

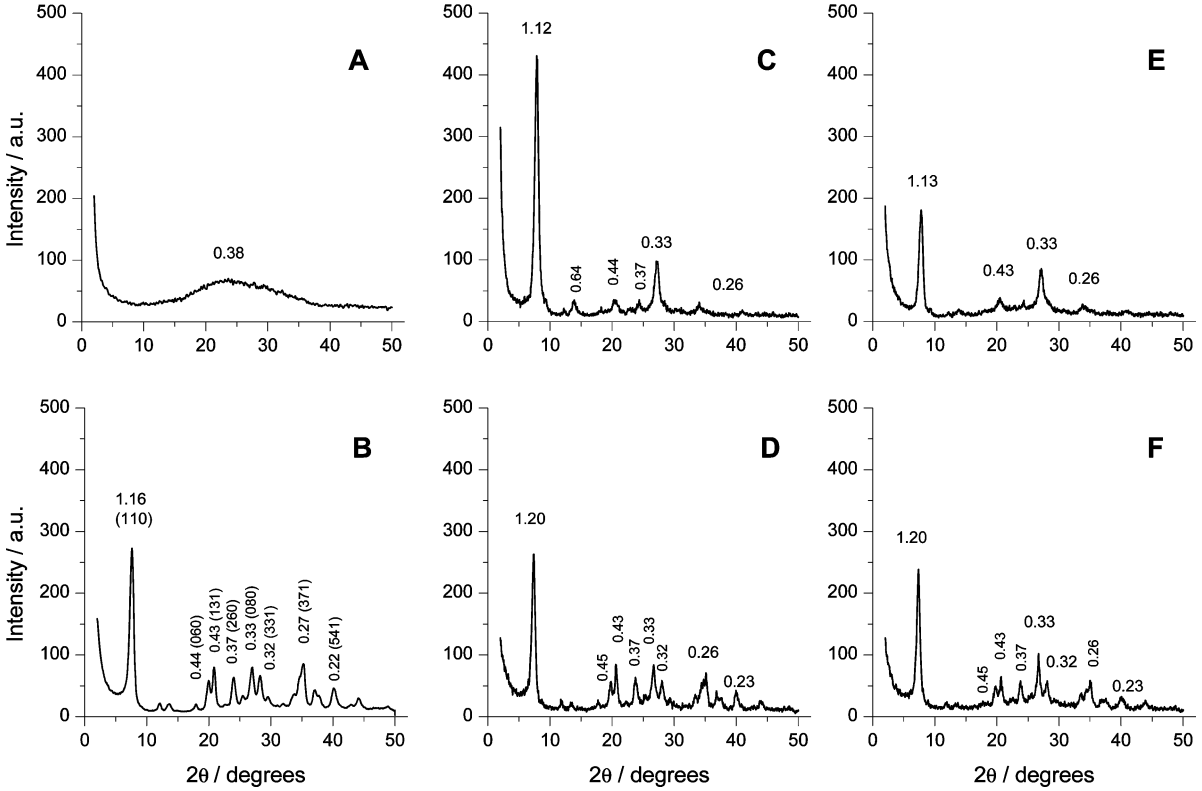

Figure 2. X-ray diffraction patterns of (A) chitosan, (B) pristine sepiolite, and the chitosan−sepiolite nanocomposites prepared from mixtures containing (C, D) 10.7 g chitosan/100 g sepiolite and (E, F) 42.9 g chitosan/100 g sepiolite. Parts C and E correspond to N-WN samples, while D and F are the diffractograms of WN samples. (All values in graphs are in nanometers).

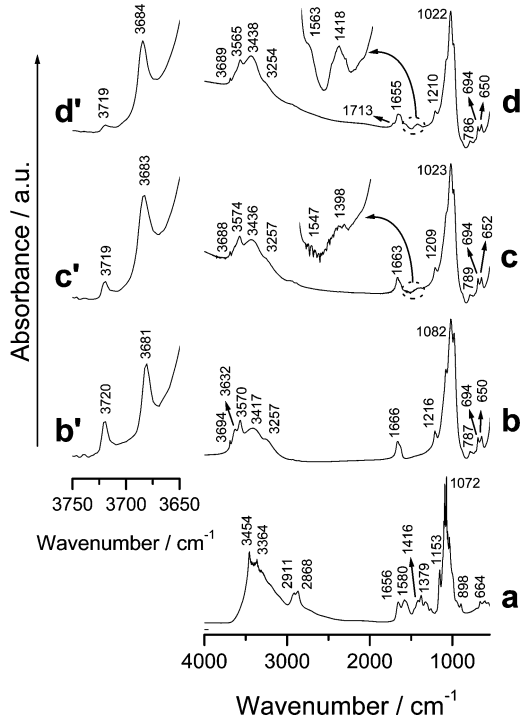

Figure 3. FTIR spectra in the 4000−550 cm^{-1} region of the pristine chitosan (a), the starting sepiolite (b), and the chitosan−sepiolite samples prepared from a mixture containing 42.9 g of chitosan per 100 g of sepiolite: the WN sample with 72.0 mequiv chitosan/100 g (c) and the N-WN sample with 94.8 mequiv chitosan/100 g (d). Spectra were recorded on KBr pellets except for chitosan (film). Spectra in the 3750−3650 cm^{-1} region correspond to sepiolite (b′), the WN sample (c′), and the N-WN sample (d′) (recorded on film samples).

In contrast, for N-WN samples some of the vibration bands attributed to chitosan can be observed, while others are overlapped by the characteristic bands of sepiolite. The band assigned to the protonated amino group (δ_{NH3}) is also shifted toward a lower wavenumber in the nanocomposite spectrum (1563 cm^{-1}), this effect being attributed to the electrostatic interaction of the positively charged amino groups of chitosan with the negatively charged sites of the sepiolite.

We have invoked the formation of chitosan multilayer arrangements on the external sepiolite surface, due to the high tendency of this biopolymer to form lamellar aggregates and their stability being assured by strong hydrogen bond intermolecular interactions. The existence of hydrogen bond interactions between chitosan and the silicate surface could be evidenced by IR spectroscopy (Figure 3b′−d′), showing the perturbation (intensity loss) by hydrogen bonding of the band at 3720 cm^{-1} assigned to the stretching OH vibrations silanol groups located at the external surface of sepiolite[16,20,27] due to their interaction with the adsorbed chitosan. It is known that the perturbation of this band produces a shift toward low-frequency values that are not observed in the spectrum due to the overlapping with stretching OH bands of water molecules.[20] The intensity decrease of the silanol band in different extent can be correlated with the surface coverage degree. In contrast, the band assigned to the stretching OH vibration of Mg−OH appearing at ca. 3680 cm^{-1} remains unaltered even at high amounts of adsorbed chitosan. It should be remembered that this last type of hydroxyl groups is located inside the structural blocks of sepiolite, being therefore inaccessible to adsorbed species (Scheme 1).

Solid-state high-resolution NMR spectroscopy was also applied to characterize the chitosan−sepiolite nanocomposites. The ^{13}C NMR spectrum (Figure 4b) of a N-WN sample

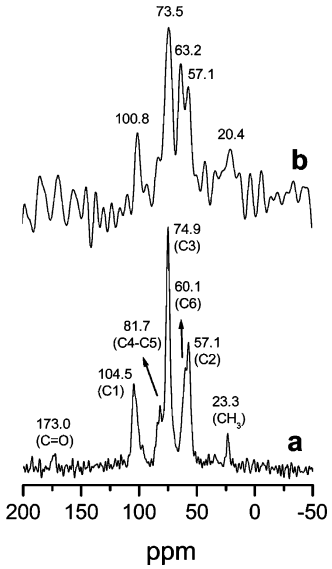

Figure 4. ^{13}C NMR spectra of (a) pure chitosan and (b) N-WN chitosan−sepiolite sample containing 110.5 mequiv of chitosan per 100 g sepiolite.

containing 110.5 mequiv chitosan/100 g shows a low signal-to-noise ratio and broader peaks than those observed in the starting chitosan (Figure 4a), indicating strong polymer−clay interactions. The signals at 104.5, 57.1, 74.9, 81.7, and 60.1 ppm are assigned to C1, C2, C3, C4−C5, and C6, respectively, in the chitosan piranose rings.

The LT-SEM technique allows the quenching SEM images of samples with high water content at low temperature. Scanning electron micrographs of the 3% (w/v) Pangel S9 and the chitosan−sepiolite suspensions, frozen by immersion of a sample drop in liquid nitrogen before drying the nanocomposites, are shown in Figure 5. In the absence of chitosan (Figure 5a), dispersed sepiolite fibers are clearly observed. In contrast, SEM images corresponding to the chitosan−sepiolite nanocomposites prepared from solutions containing initially 2.68 g and 100 g of chitosan/100 g sepiolite (parts b and c of Figure 5, respectively) show an agglomeration of the sepiolite fibers due to the adsorption of chitosan, this effect becoming stronger as the amount of adsorbed biopolymer increases. In these conditions, the sepiolite fibers seem to be tightly integrated within the biopolymer structure, providing compactness to the corresponding bio-nanocomposites. Such arrangement of silicate fibers and biopolymer slabs suggests the enhancement of mechanical and barrier properties of these nanocomposites.

Ion-Exchange Behaviors. To ascertain the ionic exchange behavior of the resulting chitosan−sepiolite nanocomposites, we have developed an innovative procedure consisting of the study of their electrical response by application of direct potentiometry. As predicted by the Nernst equation (eq 1), ideally the potential of a selective electrode should be a linear function of the logarithm of the ion activity:[33]

$$E = E^\circ + \frac{RT}{z_i F}\ln a_i = E^\circ + \frac{59.16}{z_i}\log a_i \qquad (1)$$

(33) Brett, C. M. A.; Oliveira Brett, A. M. Potentiometric sensors. In *Electrochemistry: principles, methods and applications*; Oxford University Press Inc.: New York, 1993; pp 289−309.

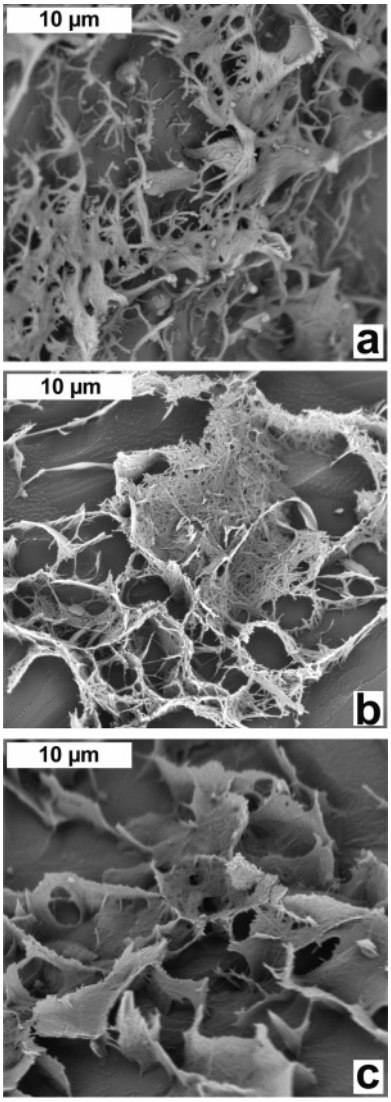

Figure 5. Low-temperature scanning electron microscopy images of 3% (w/v) Pangel S9 (a) and suspensions with 2.68 g (b) and 100 g (c) of chitosan per 100 g of sepiolite.

where E is the electrode potential, E° the reference potential, R the gas constant, T the thermodynamic temperature, F the Faraday constant, a_i the ion activity, and z_i the charge number of the ion.

Given that the charge of the measured ions is involved in the Nernst equation, the slope of potential vs log a_i changes according to its nature, i.e., anionic or cationic, and also for mono- or polyvalent ions. Thus, the predominance of anionic or cationic exchange sites in the chitosan−sepiolite nanocomposites, and in consequence the higher affinity of each material toward anions or cations, will tune the potentiometric response of the resulting systems. For this purpose, carbon paste electrodes (CPEs) were modified with the chitosan−sepiolite samples and their potentiometric responses were evaluated in NaCl solutions of increasing concentration. For comparison, modified CPEs were prepared with the pristine sepiolite, which give slope values of +18.2 mV/decade.

As shown in Figure 6A, all the CPEs prepared with WN samples, where the excess of chitosan has been removed, show positive slopes ranging between +15 and +19 mV/decade, indicating the behavior of the hybrid material as a

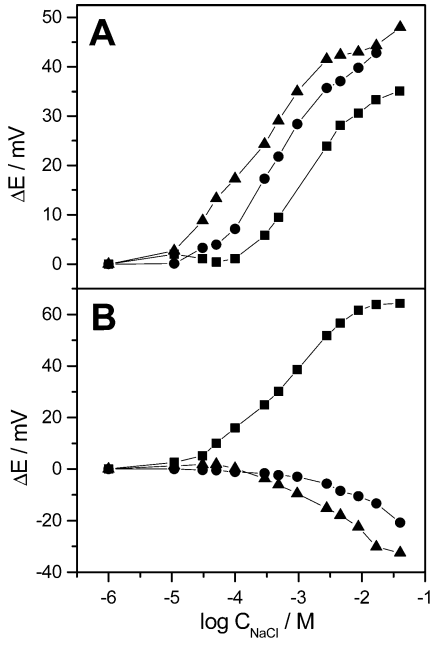

Figure 6. Potentiometric responses of the CPEs modified with (A) WN samples containing (■) 43.5, (●) 51.3, and (▲) 72.0 mequiv chitosan per 100 g of sepiolite and with (B) N-WN samples containing (■) 45.6, (●) 50.7, and (▲) 94.8 mequiv chitosan per 100 g of sepiolite. The potential was measured in NaCl solutions of increasing activity against a Ag/AgCl reference electrode.

cationic exchanger. In contrast, modified electrodes based on N-WN samples could exhibit positive or negative slopes depending on the amount of chitosan interacting with the silicate (Figure 6B). For high amounts of adsorbed chitosan, a negative slope is obtained, indicating that the cationic exchange capacity of sepiolite has been reversed to an anionic exchange character due to the presence of available protonated amino groups.

On the basis of the observed response of the nanocomposites, they could be envisaged in a first approach for further applications as the active phase of potentiometric sensors for ions detection in aqueous solutions, in a way similar to that reported for chitosan−montmorillonite materials.[7] However, in this case the chitosan−sepiolite based CPEs showed a low stability in performance, and therefore, this electrode design (CPE configuration) cannot be employed for such applications. It could be appointed that alternative electrode designs based in epoxy or PVC matrixes, which give more robust devices, can be a potential solution for the proposed electroanalytical applications.

It is known that the pH value of a sepiolite suspension varies with time reaching a basic value, due to the lixiviation of Mg ions that are replaced by H^+ from water. Thus, the pH value of a 0.2% (w/v) sepiolite suspension was measured, showing a variation from 5.9 to 8.8 in few minutes (Figure 7). Both the WN chitosan−sepiolite samples and the sepiolite previously treated in acetic acid show a similar effect, with a pH change from 5.9 to 7.4 and 6.8, respectively. Probably, the final value in both cases is less basic because a partial lixiviation of Mg ions has already taken place in the previous preparation step. In contrast, N-WN samples show a different behavior, and in 0.2% (w/v) suspensions of these samples the pH value is kept practically constant at 4.9−5.0. This fact agrees with the result provided by direct potentiometry,

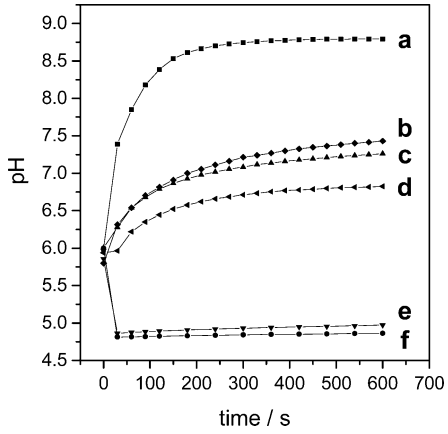

Figure 7. Variation of pH as a function of time in 0.2% (w/v) suspensions of pristine sepiolite (a), the WN samples containing 72.0 (b) and 51.3 mequiv/100 g (c), sepiolite treated in 1% acetic acid for 24 h (d), and the N-WN samples containing 94.8 (e) and 50.7 mequiv/100 g (f).

pointing out the presence of an excess of protonated amino groups that are responsible for the new behavior of these samples as anionic exchangers. In fact, the theoretical pH value estimated for a N-WN suspension, taking in consideration the chitosan amount adsorbed onto sepiolite as well as the acidity constant of amino groups in chitosan (pK_a = 6.3),[34] results in a value of 4.9, which matches with the measured value.

On the basis of both type of experiments, the direct potentiometry and the measurement of pH, the presence of protonated amino groups can be confirmed, indicating that the N-WN chitosan−sepiolite samples can be employed as a H^+ reservoir in different applications. As these materials can be easily conformed as membranes showing good mechanical properties, the proton conductivity could be of great interest for applications in fuel-cell devices. However, the values of H^+ conductivity initially tested in these membranes are too low for this kind of use, and the system must be further improved by incorporation of stronger acidic agents.

Thermal Stability. DTA and TG curves recorded in the 20−1000 °C range under air flow conditions (Figure 8) point out the thermal stability of the chitosan−sepiolite nanocomposites in comparison to the biopolymer alone. The DTA curve corresponding to the pristine chitosan shows an endothermic process at 63 °C and two exothermic processes at 317 and 566 °C, respectively. The first one, associated with a weight loss of 8.6% in the TG curve, is attributed to the loss of physically adsorbed water molecules. The exothermic processes at 317 °C (weight loss of 59%) and 566 °C (weight loss of 33%) are related to the pyrolytic decomposition followed by the combustion of the biopolymer.[35,36]

The stabilizing effect of the chitosan adsorption onto sepiolite is clearly observed in Figure 8b, corresponding to a WN sample with 72.0 mequiv/100 g prepared from a

(34) Muzzarelli, R. A. A. Modified Chitosans and their Chromatographic Performances. In *Proceedings of the First International Conference on Chitin/Chitosan*; Muzzarelli, R. A. A., Pariser, E. R., Eds.; Massachusetts Institute of Technology: Boston, 1978; pp 335−354.
(35) Zohuriaan M. J.; Shokrolahi, F. *Polym. Test.* **2004**, *23*, 575−579.
(36) Waymack, B. E.; Belote, J. L.; Baliga, V. L.; Hajaligol, M. R. *Fuel* **2004**, *83*, 1505−1518.

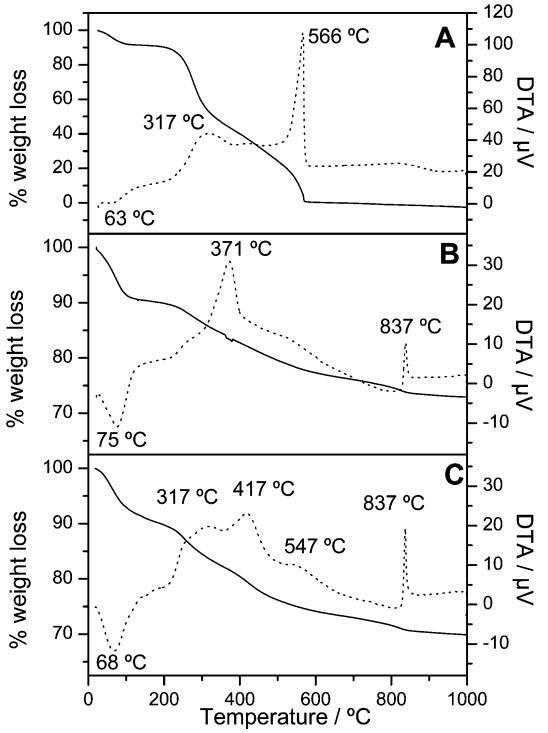

Figure 8. TG and DTA curves obtained for the pristine chitosan (A), and the chitosan−sepiolite samples prepared from 42.9 g chitosan/100 g sepiolite: WN sample (B) and N-WN sample (C).

starting mixture of 42.9 g of chitosan/100 g sepiolite. The DTA peaks corresponding to chitosan decomposition have been shifted toward higher temperature values, appearing at 371 °C, being associated with a weight loss of 10.4%. The water content of this nanocomposite is 9.5% at ca. 75 °C, due to the hydrophilic character of both components, chitosan and sepiolite. The DTA peak at 837 °C corresponds to the dehydroxylation process of the residual sepiolite.[37]

The related N-WN sample, prepared from the same starting mixture and containing a great excess of chitosan (94.8 mequiv/100 g), shows additional peaks in the DTA curve (Figure 8c) in comparison with that of the WN sample. In addition to the endothermic peak at 68 °C related to the loss of water (8.9%) and the exothermic peak at 837 °C due to the clay substrate under heating, three exothermic processes are observed. Among them, peaks at 317 and 547 °C appear at similar values to those reported for the pristine biopolymer (Figure 8a) and could be related to the excess of chitosan that is not tightly bound to the clay substrate. In contrast, the process at 417 °C may be attributed to the decomposition (pyrolysis + combustion) of adsorbed chitosan, as above indicated for the nanocomposite without excess of chitosan. As mentioned above, this increment in the temperature required for the thermal decomposition of chitosan points out the improved thermal stability of the resulting chitosan−sepiolite nanocomposites.

Mechanical Properties. The elasticity modulus was obtained for the WN and N-WN samples, conformed as films, from the linear zone of the tension vs deformation representation. In Table 1 are collected the values obtained for the different nanocomposites. The value of elasticity modulus of sepiolite is not included as the films of such silicate show great fragility, thus such measurements were avoided. The starting chitosan prepared as thin films (0.008 ± 0.002 mm) gives an elasticity modulus of 1.5 ± 0.4 GPa.

An improvement of the mechanical properties of both the WN and the N-WN samples with respect to the starting components, sepiolite and chitosan, is clearly observed. In fact, the measured samples show the typical synergic behavior of polymer−clay nanocomposites, in which the mechanical properties of the components associated at the nanometer level are superior to those of the components measured separately. As observed in the LT-SEM images, the chitosan seems to act as an adhesive connecting the sepiolite fibers, and such a strong interaction between both components could be the reason of the enhancement of the elasticity modulus in the nanocomposite samples. The measured values agree with those reported by other authors for the interaction of chitosan with hydroxyapatite as inorganic filler (see Hu et al.).[38] In that case, the hybrid materials processed as a bioabsorbable implant to promote new bone formation showed a Young's modulus of 3.4 GPa.

We have observed that WN samples show a linear relationship between the modulus and the amount of adsorbed chitosan (Figure 9a), contrary to that observed for the N-WN samples (Figure 9b). Such a behavior could be attributed to the low homogeneity observed in these last samples, especially in N-WN samples with a high amount of chitosan associated with the sepiolite substrate. The total error in the measurements can be mainly ascribed to the error due to the film's thickness determinations, being higher in the WN samples that show lower thickness values (Table 1).

Conclusions

An example of biohybrid materials based on natural, abundant, low-cost, and environmentally friendly resources is here reported. The interaction of sepiolite with the cationic biopolymer chitosan results in nanostructured biohybrid materi-

Table 1. Composition, Dimensions, and Elasticity Modulus of the Chitosan−Sepiolite Samples

	washed samples				nonwashed samples			
starting amounts (g chitosan/ 100 g sepiolite)	chitosan coverage (mequiv chit/ 100 g sepiolite)	thickness (mm)	width (mm)	*E* (GPa)	chitosan coverage (mequiv chit/ 100 g sepiolite)	thickness (mm)	width (mm)	*E* (GPa)
2.68	43.5	0.044 ± 0.002	6.07 ± 0.01	1.6 ± 0.1	45.6	0.096 ± 0.002	6.02 ± 0.01	3.0 ± 0.1
10.7	51.3	0.025 ± 0.002	6.06 ± 0.01	4.5 ± 0.4	50.7	0.095 ± 0.002	5.98 ± 0.01	3.6 ± 0.1
21.5	80.2	0.030 ± 0.002	6.14 ± 0.01	3.7 ± 0.2	77.7	0.117 ± 0.002	6.11 ± 0.01	3.2 ± 0.1
32.2	76.1	0.026 ± 0.002	6.10 ± 0.01	4.1 ± 0.3	83.1	0.115 ± 0.002	5.86 ± 0.01	6.5 ± 0.1
42.9	72.0	0.015 ± 0.002	5.98 ± 0.01	3.3 ± 0.4	94.8	0.082 ± 0.002	6.15 ± 0.01	4.3 ± 0.1
53.7	75.2	0.038 ± 0.002	6.00 ± 0.01	3.2 ± 0.2	110.5	0.166 ± 0.002	6.05 ± 0.01	3.1 ± 0.1
64.4	91.1	0.013 ± 0.002	6.05 ± 0.01	5.1 ± 0.8	141.1	0.090 ± 0.002	6.01 ± 0.01	3.9 ± 0.1

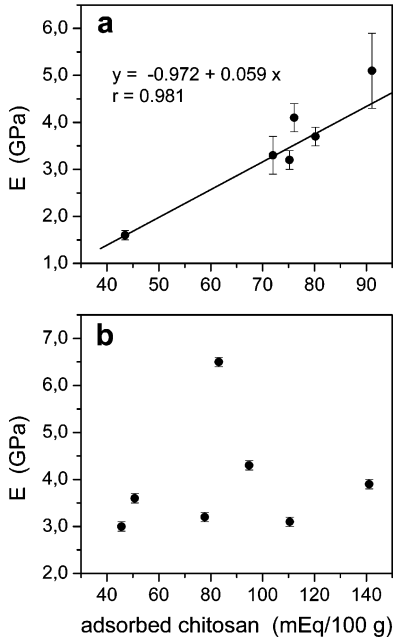

Figure 9. Elasticity modulus as a function of the amount of chitosan adsorbed onto sepiolite in (a) WN and (b) N-WN samples.

als provided with enhanced mechanical properties. The strong interaction between both the organic and the inorganic moieties is confirmed by several characterization techniques, including FTIR, LT-SEM, and dynamic mechanical analysis. The thermal stability of the chitosan−sepiolite nanocomposites is also increased with respect to the pristine biopolymer.

Direct potentiometry has been applied for the first time, to the best of our knowledge, as a tool to ascertain the ionic exchange character of the resulting chitosan−sepiolite nanocomposites. In addition, from the measurement of the pH value in suspensions of these nanocomposites, it has been stated that these chitosan−sepiolite samples are a reservoir of H^+, providing an acidic environment. The measured modulus in all the prepared samples confirms the enhancement of their mechanical properties with respect to the clay or the polymer taken separately, due to the strong interaction between the chitosan and the sepiolite substrate. Thus, the new chitosan−sepiolite hybrid materials are processed as self-supporting films that could potentially be used in different applications such as separation processes of gas mixtures, components for electrochemical sensors, or membranes in fuel-cell devices.

Acknowledgment. This work was supported by the CICYT (Spain; Project MAT2003-06003-C02-01) by the Comunidad de Madrid (Spain; Project S-0505/MAT/000227) and by the Junta de Andalucía (Spain; Project IFAPA-2002.000890). M.D. acknowledges the CSIC for an I3P postdoctoral contract. We also thank F. Pinto for technical assistance in LT-SEM studies and Dr. I. Sobrados for her assistance in NMR studies.

CM0523642

(37) Balci, S. *J. Chem. Technol. Biotechnol.* **1996**, *66*, 72−78.
(38) Hu, Q.; Li, B.; Wang, M.; Shen, J. *Biomaterials* **2004**, *25*, 779−785.